Journal of Power Sources 241 (2013) 460–466

Contents lists available at SciVerse ScienceDirect

Journal of Power Sources

journal homepage: www.elsevier.com/locate/jpowsour

Facile chemical synthesis of nitrogen-doped graphene sheets and their electrochemical capacitance

Xusheng Du [a,*], Cuifeng Zhou [b], Hong-Yuan Liu [a], Yiu-Wing Mai [a], Guoxiu Wang [c]

[a] Center for Advanced Materials Technology (CAMT), School of Aerospace Mechanical & Mechatronic Engineering, J07, The University of Sydney, NSW 2006, Australia
[b] WPI Center for Materials Nanoarchitectonics (MANA), National Institute for Materials Science (NIMS), Tsukuba, Ibaraki 3050044, Japan
[c] Centre for Clean Energy Technology, School of Chemistry and Forensic Science, University of Technology, Sydney, NSW 2006, Australia

HIGHLIGHTS

- N-doped graphene (NGS) is simultaneously reduced from GO and functionalised at 80 °C.
- The reduction and N-doping of GO occur in 1 wt.% ammonia water at atmosphere pressure (101,325 Pa).
- NGS has a N composition of 4.4 at.% and exhibits higher thermal stability than GO.
- Specific capacitance of NGS is nearly twice that of RGO without N-doping.
- NGS exhibits a maximum specific capacitance of 233.3 F g^{-1} and superior cycling stability.

ARTICLE INFO

Article history:
Received 18 February 2013
Received in revised form
10 April 2013
Accepted 27 April 2013
Available online 9 May 2013

Keywords:
Nitrogen doping
Graphene
Specific capacitance
Functionalization
Reduced graphene oxide

ABSTRACT

To improve the electrochemical performance of graphene materials, nitrogen-doped graphene sheets (NGS) were simultaneously reduced and functionalized with nitrogen (N) doping from graphene oxide (GO) by a simple process using 1 wt.% ammonia water solution as the reducing agent, nitrogen precursor and solvent. The NGS were characterized by X-ray diffraction, X-ray photoelectron spectroscopy, transmission electron microscopy–energy dispersive spectroscopy microanalysis, and differential scanning calorimetry. The thermal stability of NGS was much higher than that of GO. The N content in NGS was 4.4 at.% and a maximum specific capacitance up to 233.3 F g^{-1} was obtained at 0.5 A g^{-1}. At 0.02 V s^{-1}, the NGS exhibited a specific capacitance of 140.3 F g^{-1}, which was over 8 times that of GO and nearly 2 times that of graphene without N-doping. These results revealed that N-doping of functional graphene provide remarkable improvements on the electrochemical capacitive performance of graphene materials. The NGS also showed high cycle stability of capacitive performance.

1. Introduction

Recently, the development of capacitors with high energy and power densities, and lower fabrication costs have attracted much interest due to the growing demand for portable electric systems and hybrid electric vehicles. Carbon materials are common electrode materials for electrochemical capacitors [1–3]. To improve their electrochemical performance, the introduction of a heteroatom, such as nitrogen (N), has been verified as a promising approach. Two conventional methods have been usually used to synthesize N-doped carbon materials. One is by direct N-doping during the growth of the carbon materials [4–7], and another is by thermal treatment of the N-containing polymers [8–11]. A high temperature environment is often required for both methods, and thermally stable products with poor wettability and low chemical activity are always obtained. Besides these two methods, the introduction of nitrogen into carbon materials can also be achieved by modifying the N-containing organic groups through a wet chemical method, which usually comprises two steps: (a) creation of carboxylic acid groups on the surface of carbon materials; and (b) amidation [12–14]. Compared to pristine carbon materials, nitrogen-modified carbon products obtained by this method have higher chemical activity and affinity to other molecules and polymer systems.

As a recently developed carbon material, graphenes have attracted increasing attention owing to their two-dimensional nanostructure, extraordinary electrical and thermal characteristics, superior

* Corresponding author. Fax: +61 2 93513760.
E-mail address: xdu@usyd.edu.au (X. Du).

0378-7753/$ – see front matter © 2013 Elsevier B.V. All rights reserved.
http://dx.doi.org/10.1016/j.jpowsour.2013.04.138

mechanical properties, and potential low production cost. These functional properties render them suitable materials for many advanced engineering applications [15–19], such as electrode materials for high performance electrochemical capacitors. Graphenes can be prepared by the chemical reduction of graphene oxide (GO) with many reducing agents, e.g., hydrazine [19–21], sodium borohydride [22,23] and ethylene glycol (EG) [17,18]. It is well known that these chemicals are hazardous to human health and the environment; for example, hydrazine, hydrazine hydrate and sodium borohydride are highly poisonous and explosive materials [24]. Hence, it is desirable to achieve GO reduction by more environment-friendly agents, and to prepare functional graphenes with high electrochemical performance by N-doping. Two main methods have been developed to achieve this goal. One is by thermal treatment of GO with urea at high temperature, normally above 600 °C [25,26]. Another is by hydro- or solvo-thermal treatment of GO in the presence of concentrated ammonia water [27] or organoamine [28]. Although hydro- or solvo-thermal reaction can occur at lower temperature (normally over 100 °C), the pressure of the reaction system inside of the autoclave is inevitably much higher than that of the outside and is sometimes difficult to control. Herein, a simple and mild method to fabricate N-doping of graphenes directly from GO in a very dilute ammonia water (~1 wt.%) is presented. With this method, the reduction of GO with ammonia water and the N-doping of graphene are expected to be achieved simultaneously under mild experimental conditions. The method is distinctly different to previous reported solvo-thermal treatment of GO with EG and ammonia water [17], where EG is used as reducing agent and solvent, and ammonia water serves merely as nitrogen precursor. More importantly, the preparation reaction can be conducted only at 80 °C at atmosphere pressure (that is, 101,325.00 Pa), a much milder experimental condition compared to the high temperature at 180 °C in an autoclave with unknown pressure [17,27,28]. Also, a very high concentration of ammonia water (28 wt.%) is used in the hydrothermal method [27]. Since all these previous methods to N doped graphene sheets (NGS) require energy-intensive batch process and special equipment or expensive reagents, the present method is, by contrast, energy-efficient, economical and capable of industrial scale-up. The capacitance performance of NGS has been studied mainly in alkaline solutions [26–28]. In this work, the electrochemical capacitive behaviour of NGS in acid electrolyte will be investigated. To study the effect of the chemical reduction and N-doping on the electrochemical performance of graphene materials, GO and reduced GO using sodium borohydride will also be prepared and their electrochemical properties compared with those of NGS.

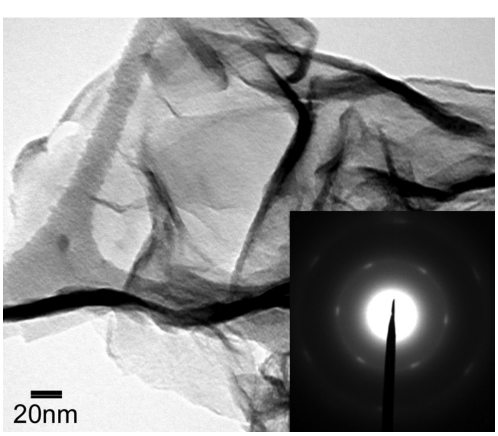

Fig. 1. Transmission electron microscopy image of NGS. Inset is its selected area electron diffraction pattern.

2. Experimental

2.1. Materials

Graphene oxide was prepared from natural graphite powder using a modified Hummers [29] method. 10 g of graphite powder was mixed with 230 mL cold (at 0 °C) concentrated H_2SO_4 (98 wt.%). Then, 30 g $KMnO_4$ was added gradually into the mixture with stirring and cooling to keep below 20 °C. Subsequently, the final mixture was stirred around 35 °C for 0.5 h. 460 mL distilled water was then added slowly and the mixture was held at ~98 °C for 0.25 h. The reaction was terminated by adding 1400 mL distilled water and 100 mL 30 wt.% H_2O_2 solution. The mixture was filtered and successively washed with 5 wt.% HCl aqueous solution until no sulphate could be detected with $BaCl_2$ and then dried at 60 °C in a vacuum oven.

To prepare N-doped graphene, 0.25 g GO was added to 260 mL of ~1 wt.% ammonia water (diluted from 28 wt.% ammonia water with distilled water) via ultra-sonication. This solution was stirred at 80 °C for 6 h. After the reaction, the solution was filtered and the

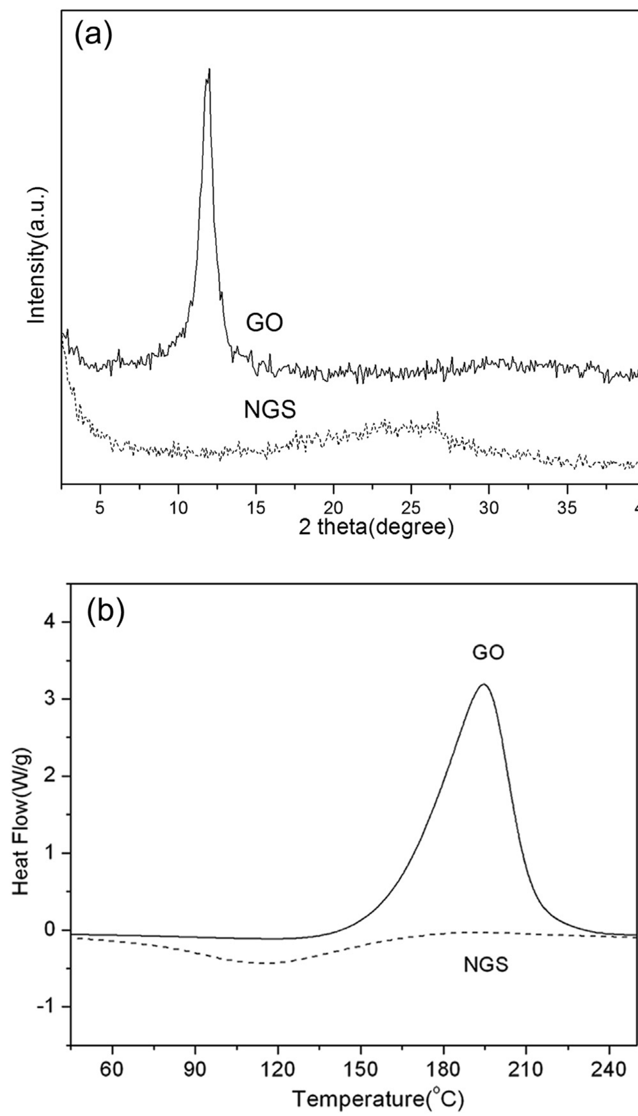

Fig. 2. (a) X-ray diffraction patterns; and (b) differential scanning calorimetry curves of GO and NGS.

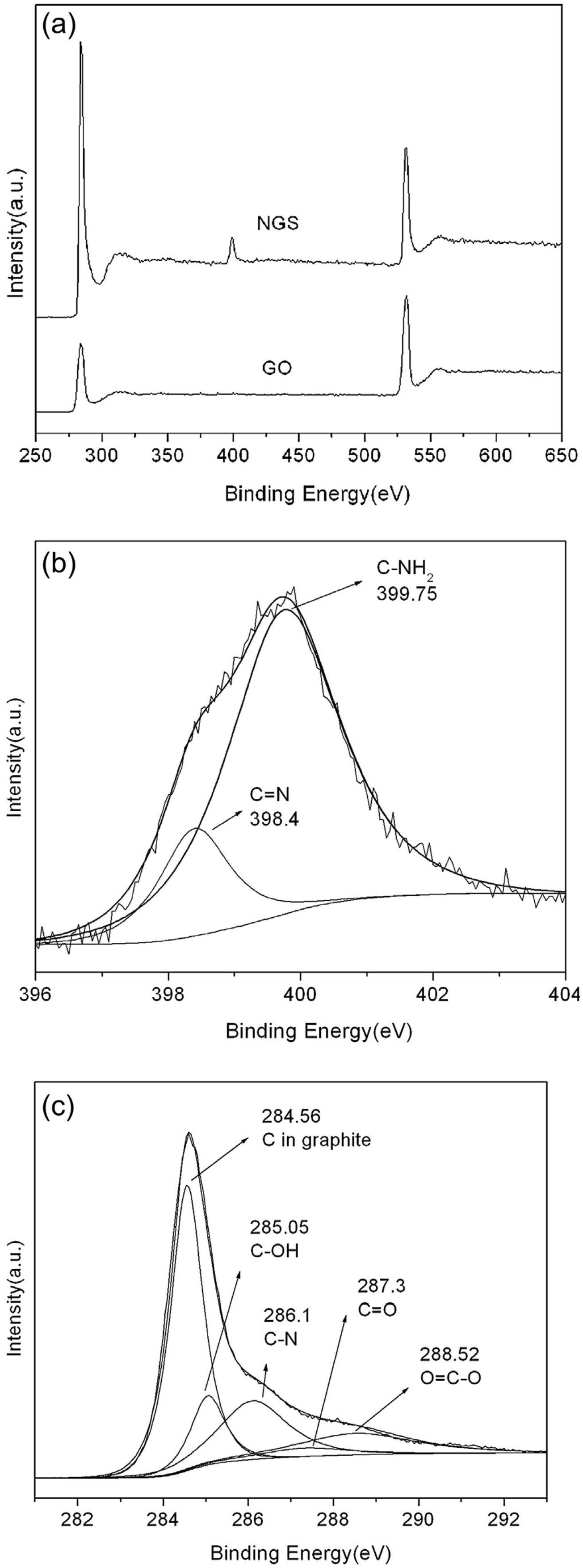

Fig. 3. (a) X-ray photoelectron spectroscopy spectra for NGS and GO; (b) N1s spectrum of NGS; and (c) C1s spectrum of NGS.

filter cake was repeatedly washed with distilled water, and dried in an oven at 80 °C for 24 h for further use. For comparison, borohydride-reduced GO was also fabricated from GO. Briefly, 2 g GO in 200 mL distilled water was sonicated for 0.5 h and 6 g $NaBH_4$ in 100 mL water was added to the mixture and stirred for another 0.5 h. Subsequently, the final mixture was stirred around 80 °C for 2 h. The reduced GO was obtained after filtration, washed with distilled water and dried at 60 °C in a vacuum oven for 24 h.

2.2. Characterization and measurements

X-ray diffraction (XRD) patterns were obtained from tests conducted using an X-ray diffractometer (Siemens D5000) with Ni-filtered Cu Kα radiation (λ = 1.54 Å). Transmission electron microscopy (TEM) was performed on a Philips CM12 (120 kV) and transmission electron microscopy–energy dispersive spectroscopy (TEM–EDS) microanalysis with a JEOL 2200FS (200 kV). Differential scanning calorimetry (DSC) data were recorded with a TA modulated DSC 2920 instrument in a nitrogen atmosphere. An X-ray photoelectron spectroscopy (XPS) system, (SPECS-XPS, Germany) was used to analyze the element concentration and binding energies of the samples. The XPS system was equipped with a high sensitivity PHOIBOS 150-9 MCD energy analyser and an Al Kα X-ray source (1486.74 eV) was used.

Electrochemical characterisations were conducted on an Electrochemical Analyzer (CH Instruments). All the solutions were prepared in distilled water and the potentials reported were all referenced to a saturated calomel electrode (SCE). A three-electrode electrochemical cell was used for the measurements, where the counter electrode was a Pt foil and the reference electrode was a SCE. The sample was dispersed into 2 mL ethanol and sonicated for several hours in order to prepare a graphene suspension. The working electrode was fabricated by casting the graphene ink onto a 3 mm diameter glassy carbon electrode followed by another coating with a 2-propanol solution containing 1 wt.% Nafion to fix the material on the electrode surface. The loading of the active materials on the electrode was 0.28 and 0.08 mg cm^{-2} for the galvanostatic charge/discharge and cyclic voltammogram tests, respectively. Electrochemical impedance spectroscopy (EIS) measurements were made in the frequency range of 0.1–100,000 Hz by applying an AC voltage with 10 mV perturbation. Prior to the electrochemical measurements, the coated electrode was soaked in a 1 M H_2SO_4 solution for at least 2 min.

3. Results and discussion

The N-doped graphene sheets were prepared by a one-step process of reduction of GO and simultaneous introduction of N at a relatively low temperature (80 °C) with a reaction time of 6 h. In this method, ammonia water took the roles of reducing agent and nitrogen precursor for dispersion of graphitic nanosheets. After the reaction was finished, the solution of GO turned from dark brown to deep black, indicating the reduction of GO after the treatment.

TEM image of the sample (Fig. 1) reveals that the resulted graphene sheets have many scrolls and/or folds on the sheets, which may be due to their large aspect ratio and the presence of organic groups on the surfaces of the sheets. The as-obtained NGS can be well-dispersed in polar solvents, such as water, ethanol and *N*,*N*-dimethylformamide. The selected area electron diffraction of the NGS displays a typical hexagonal lattice pattern (see inset in Fig. 1), which is similar to that of graphene from GO reduced by $NaBH_4$ [23]. Transmission electron microscopy–energy dispersive spectroscopy mapping also confirms the uniform dispersion of N on the graphene sheets (see Fig. S1 in Supporting Information).

The X-ray diffraction patterns of GO and NGS are shown in Fig. 2a. Graphene oxide exhibits a sharp (001) diffraction peak at 11.8°, corresponding to an interlayer spacing of 0.75 nm. After the reaction with ammonia water at 80 °C, the crystalline structure of GO is significantly changed and no dominant peak observed in GO can be found for NGS, implying the complete loss of the periodic structure of GO and almost no ordered restacking of the functionalized graphene sheets. This result is different from that of graphene obtained from the solvo-thermal reaction of GO with ammonia water in EG at 180 °C in an autoclave [17], where the graphene displays a (001) peak at 12.48° (larger than that of the pristine GO at 11.72°), hence indicating a decreased interlayer spacing of the graphitic sheets after the solvo-thermal reaction in EG. By contrast, GO treated with primary alkylamine exhibits an enlarged *d*-spacing owing to the insertion of the long alkyl chains [30]. Obviously, the exfoliation of NGS achieved here will increase the enhancement of their electrochemical performance and the reinforcing effect in polymer composites since every single graphene sheet is put to its best use. The DSC curves of GO and NGS are shown in Fig. 2b. Graphene oxide shows one strong exothermic peak at ∼190 °C due to the decomposition of oxygen-containing organic groups on the GO sheets. By contrast, no exothermic peak is found below 250 °C in the DSC curve for NGS, implying reduced amounts of unstable oxygen-containing organic functional groups and good thermal stability of NGS. This is clearly an advantage when NGS are used as fillers to fabricate graphene/polymer nanocomposites, since its higher thermal stability will benefit processing and applications of these composite materials.

Both the atomic ratio of C, N and O and the chemical state in NGS are also analysed by XPS. Contrary to the spectra of GO, an obvious N1s peak appears at ∼399 eV in the XPS spectra of the NGS sample (Fig. 3a), indicating the introduction of N to NGS by the simple chemical treatment. From the XPS analysis, the C:O atomic ratio for NGS is ∼6:1, which is much higher than that of pristine GO (∼2:1). The increase of C:O atomic ratio indicates the de-oxygenation or reduction of GO after the chemical treatment. The C:O atomic ratio is less than those chemically reduced GO, which are 10.3:1 with hydrazine hydrate [20], and 13.4:1 with sodium borohydride as reducing agent [31]. This means that as a reducing agent, ammonia water is not as strong as hydrazine and sodium borohydride. Further, the XPS study of NGS sample shows that the atomic ratio of carbon to nitrogen is 18.5:1, confirming the successful doping of nitrogen and reduction of GO by ammonia water simultaneously. The 4.4 at.% of N in NGS is less than those of the products prepared through hydrothermal reaction in an autoclave, which is always above 6.2 at.% [27]. This can be caused by the different concentration of ammonia water, temperature and the pressure of the reaction system.

The functional groups on the surface of NGS samples introduced by N-doping were investigated. As shown in Fig. 3b, N1s spectrum of NGS can be de-convoluted to two peaks with binding energies of 398.40 and 399.75 eV, corresponding to the pyridinic and primary amine [32], respectively. The ratio between these two peaks is 1:4.5, indicating the main form of N-doping in the NGS is the primary amine. Moreover, the component at 286.1 eV in the C1s spectrum of NGS (Fig. 3c) can be ascribed to the C—N groups [17]. These observations show considerable de-oxygenation and primary amine addition. The reaction of ammonia with GO has been studied for a long time [33,34], whereby it is proven that ammonia can be reactive to the main oxygen-containing functional groups on the surface of the GO sheets, such as epoxide groups, carboxyl groups and carbonyl groups. Nitrogen from ammonia reacts easily with the

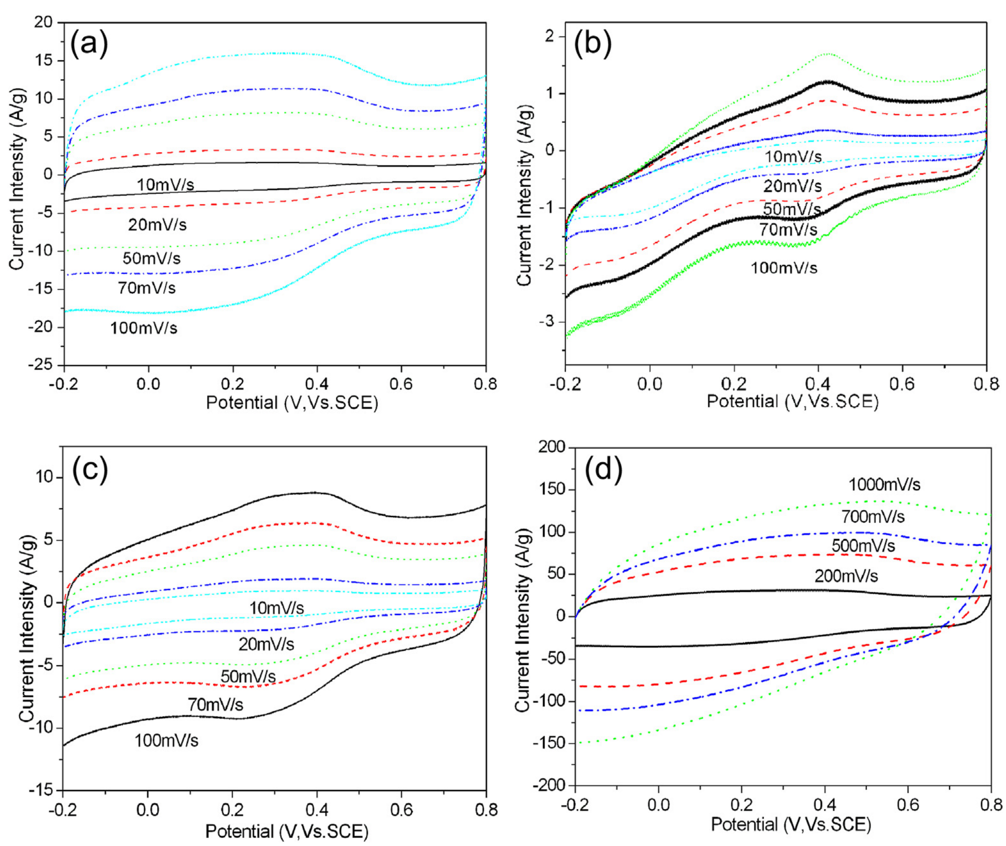

Fig. 4. Cyclic voltammograms (CV) of (a) NGS, (b) pristine GO and (c) RGO at scan rates from 10 to 100 mV s^{-1}; (d) CV of NGS at scan rates from 200 to 1000 mV s^{-1} in 1 M H_2SO_4.

carbonyl groups to give an aromatic Schiff base. The epoxide groups can react with ammonia to form primary amine and alcohol through a ring-opening reaction by nucleophilic substitution; and amide groups may also be formed after the reaction of the carboxyl groups with ammonia [33].

The electrochemical performance of NGS is enhanced greatly in comparison to GO. Similar to previously reported Nyquist plots of NGS prepared by other methods [26,27], a vertical line appears in the low frequency region in the diagram of the resulting NGS samples (Fig. S2(a)), which should be contrasted with that of GO measured in the same frequency region (Fig. S2(b)). It is generally accepted that a vertical line in the Nyquist plot indicates ideal capacitive behaviour [27]. The more vertical it is towards the imaginary y-axis, the more closely does the electrochemical cell perform as an ideal capacitor [26]. The EIS tests results indicate that NGS is much more superior to GO as the capacitor material. This is, consistent with the results of the cyclic voltammogram (CV) tests. The CV curves of NGS (Fig. 4a) show much higher pseudo-capacitance current densities than those of GO at the same scan rate (Fig. 4b). The poor electrochemical performance of GO originates from its poor electrical conductivity and low faradic reaction rate. Moreover, a pair of redox peaks appears at ~0.4 V which can be well resolved in the CV curves of GO, while such peaks are too weak to be identified in the CV curves of the NGS samples. These peaks are believed to come from the redox transition of quinine/hydroquinone in the carbon materials [18,35]. The change of resolution of these peaks after the treatment with ammonia water indicates that the oxygen-containing functionalities in GO are very much reduced in NGS, which is consistent with the aforementioned DSC (Fig. 2b) and XPS (Fig. 3a) results. To study the effect of heteroatom N-doping on the electrochemical characteristics of graphene sheets, sodium borohydride was used to reduce GO since no nitrogen was introduced to the resultant reduced graphene oxide (RGO) materials. At given scan rates, the CV curves of RGO in Fig. 4c also have much higher capacitive currents than those of GO, but much less than those of NGS. Since RGO shows similar XRD pattern as NGS (Fig. 2a) and no characteristic peak seen in GO is found in RGO (Fig. S3), the improved electrochemical performance of NGS can be attributed to the functionalization effect of N-doping, which donates electron density to the aromatic rings of the graphene sheets and increases their conductivity.

Cyclic voltammogram has been used as a typical method to evaluate the capacitance of electrode materials and the specific capacitance (Cs) can be obtained from:

$$Cs = \frac{|Q_f| + |Q_b|}{2\nu m \Delta V} \quad (1)$$

where Q_f and Q_b are the voltammetric charge (C) integrated from areas of forward and backward scans under the CV curves at different scan rates, respectively; ΔV is the potential window of charging/discharging (V), ν potential scan rate (V s^{-1}) and m mass of active electrode material (g). The capacitive current of NGS generally increases with increasing CV scan rate from 10 to 100 mV s^{-1}, as displayed in Fig. 5a. Cs of NGS calculated from these CV curves at scan rates of 20 and 100 mV s^{-1} are 140.3 and 130.5 F g^{-1}, respectively. By contrast, Cs of GO is always below 16 F g^{-1} when the scan rate is in the range of 10–100 mV s^{-1}, as calculated from Fig. 4b. The dependence of Cs of NGS on CV scan rate (Fig. 5a) indicates that NGS has good capability of capacitance retention and 93% Cs is retained as the scan rate is changed from 10 to 100 mV s^{-1}. Further increasing the scan rate, the redox peak around 0.4 V becomes more poorly resolved (Fig. 4d), showing gradual reduced contribution of the pseudo-capacitance from the

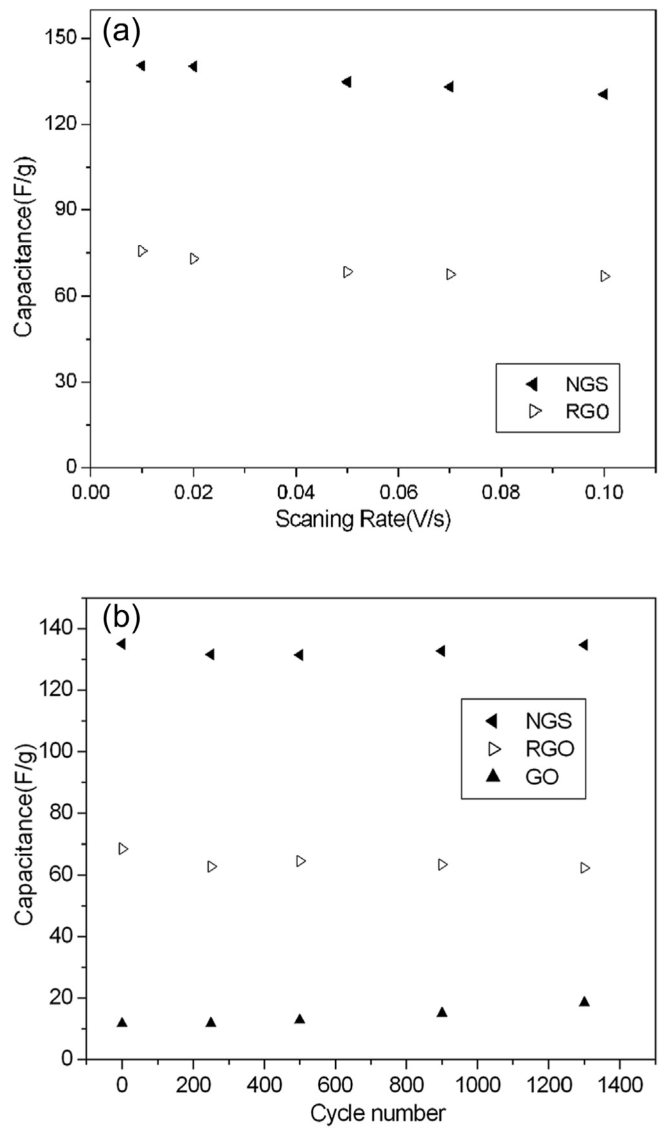

Fig. 5. Variation of specific capacitance of NGS with (a) different scan rate; and (b) a scan rate of 50 mV s^{-1}. Comparisons are made with RGO in (a) and with RGO and GO in (b).

functional groups on the NGS surface at higher CV scan rates. Therefore, the measured Cs shows a precipitous drop to 91 F g^{-1} when the scanning rate is 1000 mV s^{-1}, as calculated from the corresponding CV curve in Fig. 4d.

Similar to the CV curves of NGS, the capacitive current density of RGO decreases generally with increasing scan rate from 10 to 100 mV s^{-1} (Fig. 4c). Consequently, the calculated Cs of both NGS and RGO decrease with increasing CV scan rate from 10 to 100 mV s^{-1}, as shown in Fig. 5a. It is noted that the Cs values of NGS are much higher than those of RGO at identical scan rates. An increase of ~2 times in Cs can be achieved, confirming the advantage of the reduction and N-doping of GO with ammonia water over sodium borohydride. Moreover, NGS shows a stable Cs value of ~135 F g^{-1} at a scan rate of 50 mV s^{-1} for 1300 cycles (Fig. 5b), indicating its excellent cycle stability in sulphuric acid electrolyte for capacitor applications. RGO also exhibits a stable capacitance performance with a Cs value of ~68.5 F g^{-1} at the same scan rate. It is interesting that the Cs value of GO increases slowly from 11.7 F g^{-1} at the first cycle to 18.5 F g^{-1} at the 1300th cycles.

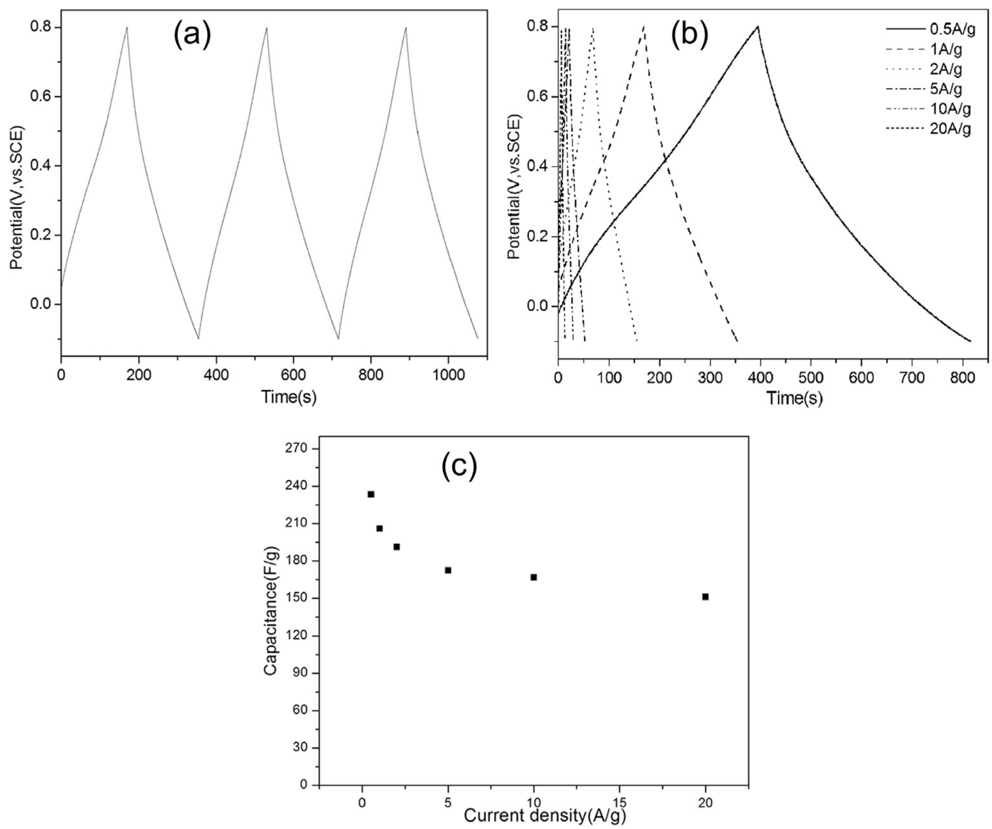

Fig. 6. Galvanostatic charge/discharge curve of NGS: (a) first 3 cycles at 1 A g^{-1} and (b) 1st cycle at different current density in 1 M H_2SO_4; and (c) dependence of specific capacitance *Cs* on the current density in the galvanostatic charge/discharge test.

Galvanostatic cycling charge/discharge measurement is another method widely used to investigate the capacitive performance of functional graphenes. With the three-electrode system, the specific capacitance *Cs* can be calculated from:

$$Cs = \frac{I\Delta t}{m\Delta V} \quad (2)$$

where I is discharge current (A), Δt discharge time (s), m weight of active electrode material (g), and ΔV discharge voltage (V). A typical galvanostatic charge/discharge curve of NGS is shown as Fig. 6a. The charge/discharge curves with different current density from 0.5 A g^{-1} to 20 A g^{-1} and the calculated *Cs* at different current densities are displayed in Fig. 6b and c, respectively. N-doped graphene sheets show an excellent specific capacitance up to 233.3 F g^{-1} at 0.5 A g^{-1}. This *Cs* value is very competitive with those of other graphenes via thermal or chemical reduction of GO by various methods [17,18,26–28,36–43], and is much higher than other common one-dimensional carbon nanomaterials, such as CNTs [44]. As expected, *Cs* decreases with increasing current density owing to the limited diffusion on the electrode surface at higher current density (Fig. 6c).

The above results obtained in this study indicate that good charge/discharge carbon sheet materials can be realized by N-doping through a facile one-step mild chemical reaction route with only ~1 wt.% ammonia water as a reducing agent, N precursor and solvent. Compared to the conventional reducing agent for GO, such as hydrazine, sodium borohydride and EG, dilute ammonia water is an economic and 'green' chemical agent that is less toxic and dangerous. Moreover, graphene has been incorporated with functional N-containing groups, showing superior electrochemical properties, and may have potential applications in other fields, such as catalyst materials and functional fillers in composites.

4. Conclusions

Graphene oxide could be reduced by 1 wt.% ammonia water at 80 °C and simultaneously functionalized with N-doping via a simple one-step process. Ammonia water was used as reducing agent, solvent, and nitrogen precursor in this process. No ordered restacking of graphene sheets was found in the resulting NGS. N-doped graphene sheets showed much higher thermal stability than GO due to the reduced content of oxygen-containing functional groups. The C:N atomic ratio in NGS was about 18.5:1. Electrochemical measurements indicated that the resulting N-doped graphene material exhibited a *Cs* of 233.3 F g^{-1} at 0.5 A g^{-1} and high cycle stability. Due to the N-doping and chemical reduction, the *Cs* of NGS nearly doubled that of RGO without N-doping and more than eight times of GO, indicating that it could be an excellent electrode material for supercapacitor applications.

Acknowledgements

X. Du and H-Y Liu acknowledge the University of Sydney for the financial support to this project through a Bridging Research Fellowship and a Bridging Support Grant, respectively.

Appendix A. Supplementary data

Supplementary data related to this article can be found online at http://dx.doi.org/10.1016/j.jpowsour.2013.04.138.

References

[1] Y. Sun, Q. Wu, G.Q. Shi, Energy Environ. Sci. 4 (2011) 1113.
[2] T. Kuila, S. Bose, A.K. Mishra, P. Khanra, N.H. Kim, J.H. Lee, Prog. Mater. Sci. 57 (2012) 1061.
[3] M. Winter, R.J. Brodd, Chem. Rev. 104 (2004) 4245.
[4] L.C. Chen, C.L. Sun, M.C. Su, L.S. Hong, O. Chyan, C.Y. Hsu, K.H. Chen, T.F. Chang, L. Chang, Chem. Mater. 17 (2005) 3749.
[5] Y.Y. Shao, J.H. Sui, G.P. Yin, Y.Z. Gao, Appl. Catal. B Environ. 79 (2008) 89.
[6] S. Dai, X.Q. Wang, J.S. Lee, Q. Zhu, J. Liu, Y. Wang, Chem. Mater. 22 (2010) 2178.
[7] N. Li, Z. Wang, K. Zhao, Z. Shi, Z. Gu, S. Xu, Carbon 48 (2010) 255.
[8] P.L. Kuo, C.H. Hsu, ACS Appl. Mater. Interfaces 3 (2011) 115.
[9] P. Zelenay, G. Wu, K.L. More, C.M. Johnston, Science 332 (2011) 443.
[10] Z.B. Lei, M.Y. Zhao, L.Q. Dang, L.Z. An, M. Lu, A.Y. Lo, N.Y. Yu, S.B. Liu, J. Mater. Chem. 19 (2009) 5985.
[11] C. Zhou, Z.-W. Liu, X.S. Du, Y.S. Yan, D.R.G. Mitchell, S.P. Ringer, Y.-W. Mai, Nanoscale Res. Lett. 7 (2012) 165.
[12] A. Gromov, S. Dittmer, J. Svensson, O.A. Nerushev, S.A. Perez-Garcia, L. Licea-Jiménez Licea, R.W. Rychwalski, E.B. Campbell, J. Mater. Chem. 15 (2005) 3334.
[13] M. Fang, Z. Zhang, J. Li, H. Zhang, H. Lu, Y.L. Yang, J. Mater. Chem. 20 (2010) 9635.
[14] C.-T. Hsieh, H. Teng, W.-Y. Chen, Y.-S. Cheng, Carbon 48 (2010) 4219.
[15] M.D. Stoller, S.J. Park, Y.W. Zhu, J.H. An, R.S. Ruoff, Nano Lett. 8 (2008) 3498.
[16] Q. Zheng, W.H. Ip, X. Lin, N. Yousefi, K.K. Yeung, Z. Li, J.K. Kim, ACS Nano 5 (2011) 6039.
[17] L. Lai, L. Chen, D. Zhan, L. Sun, J. Liu, S.H. Lim, C.K. Poh, Z. Shen, J. Lin, Carbon 49 (2011) 3250.
[18] S.Y. Yang, K.H. Chang, H.W. Tien, Y.F. Lee, S.M. Li, Y.S. Wang, J.Y. Wang, C.C.M. Ma, C.C. Hu, J. Mater. Chem. 21 (2011) 2374.
[19] D. Yu, L. Dai, J. Phys. Chem. Lett. 1 (2010) 467.
[20] S. Stankovich, R.D. Piner, X.Q. Chen, N.Q. Wu, S.T. Nguyen, R.S. Ruoff, J. Mater. Chem. 16 (2006) 155.
[21] Z. Lin, Y. Liu, Y. Yao, O.J. Hildreth, Z. Li, K. Moon, C.-P. Wong, J. Phys. Chem. C 115 (2011) 7120.
[22] H.J. Shin, K.K. Kim, A. Benayad, S.M. Yoon, H.K. Park, I.S. Jung, M.H. Jin, H.K. Jeong, J.M. Kim, J.Y. Choi, Y.H. Lee, Adv. Funct. Mater. 19 (2009) 1987.
[23] Y.-K. Yang, R.-G. Peng, C.-E. He, A. Baji, X.S. Du, Y.L. Huang, X.L. Xie, Y.-W. Mai, J. Mater. Chem. 22 (2012) 5666.
[24] M. Pumera, Energy Environ. Sci. 4 (2011) 668.
[25] Z. Lin, G. Waller, Y. Liu, M. Liu, C.-P. Wong, Adv. Energy Mater. 2 (2012) 884.
[26] K. Gopalakrishna, Kota Moses, A. Govindaraj, C.N.R. Rao, Solid State Commun. (2013), http://dx.doi.org/10.1016/j.ssc.2013.02.005.
[27] J.W. Lee, J.M. Ko, J.-D. Kim, Electrochim. Acta 85 (2012) 459.
[28] B. Jiang, C. Tian, L. Wang, L. Sun, C. Chen, X. Nong, Y. Qiao, H. Fu, Appl. Surf. Sci. 258 (2012) 3438.
[29] W.S. Hummers, R.E. Offeman, J. Am. Chem. Soc. 80 (1958) 1339.
[30] S. Stankovich, D.A. Dikin, O.C. Compton, G.H. Dommett, R.S. Ruoff, S.T. Nguyen, Chem. Mater. 22 (2010) 4153.
[31] W. Gao, L.B. Alemany, L.J. Ci, P.M. Ajayan, Nat. Chem. 1 (2009) 403.
[32] L.F. Lai, G.M. Huang, X.F. Wang, J. Weng, Carbon 48 (2010) 3145.
[33] W.H. Slabaugh, B.C. Seiler, J. Phys. Chem. 66 (1962) 396.
[34] M. Seredych, T.J. Bandosz, J. Phys. Chem. C 111 (2007) 15596.
[35] K. Zhang, L. Zhang, X. Zhao, J. Wu, Chem. Mater. 22 (2010) 1392.
[36] A.V. Murugan, T. Muraliganth, A. Manthiram, Chem. Mater. 21 (2009) 5004.
[37] Y. Wang, Z. Shi, Y. Huang, Y. Ma, C. Wang, M. Chen, Y.S. Chen, J. Phys. Chem. C 113 (2009) 13103.
[38] Y.W. Zhu, M.D. Stoller, W.W. Cai, A. Velamakanni, R.D. Piner, D. Chen, R.S. Ruoff, ACS Nano 4 (2010) 1227.
[39] W. Lv, D.M. Tang, Y.B. He, C.H. You, Z.Q. Shi, X.C. Chen, C.M. Chen, P.X. Hou, C. Liu, Q.H. Yang, ACS Nano 3 (2009) 3730.
[40] Y.X. Xu, K.X. Sheng, C. Li, G.Q. Shi, ACS Nano 4 (2010) 4324.
[41] Q.L. Du, M.B. Zheng, L.F. Zhang, Y.W. Wang, J.H. Chen, L.P. Xue, W.J. Dai, G.B. Ji, J.M. Cao, Electrochim. Acta 55 (2010) 3897.
[42] A.P. Yu, I. Roes, A. Davies, Z.W. Chen, Appl. Phys. Lett. 96 (2010) 253105.
[43] S. Biswas, L.T. Drzal, ACS Appl. Mater. Interfaces 2 (2010) 2293.
[44] S.L. Chou, J.Z. Wang, S.Y. Chew, H.K. Liu, S.X. Dou, Electrochem. Commun. 10 (2008) 1724.